A. Loarte, M. Becoulet, G. Saibene, R. Sartori, B. Alper, P.J. Lomas, W. Suttrop,
S. Jachmich, T. Eich, P. Hennequin, A. Kallenbach, G. Matthews
and JET-EFDA Contributors

Type I ELM Energy and Particle Losses in JET ELMy H-modes

Type I ELM Energy and Particle Losses in JET ELMy H-modes

A.Loarte[1], M.Becoulet[2], G.Saibene[1], R.Sartori[1], B.Alper[3], P.J.Lomas[3], W.Suttrop[4], S.Jachmich[5], T.Eich[5], P Hennequin[6], A.Kallenbach[4], G.Matthews[3] and JET EFDA Contributors*

[1]EFDA-CSU, Max-Planck-Institut für Plasmaphysik, D-85748 Garching, Germany
[2]Association Euratom-CEA, DRFC, CEA Cadarache, F-13108 St Paul lez Durance, France
[3]EURATOM/UKAEA Fusion Association, Culham, Abingdon, Oxon. OX14 3DB, UK
[4]Max-Planck-Institut für Plasmaphysik, Euratom Assoziation, D-85748 Garching, Germany
[5]Institut für Plasmaphysik, Forschungszentrum Jülich GmbH, D - 52425 Jülich, Germany
[6]Laboratoire PMI, Ecole Polytechnique, 91128 Palaiseau, France
*See appendix of the paper by J.Pamela "Overview of recent JET results",
Proceedings of the IAEA conference on Fusion Energy, Sorrento 2000

INTRODUCTION

The Type I ELMy H-mode regime is the reference regime of next step devices such as ITER. Discharges that fulfil the ITER requirements in terms of energy confinement, β_N and plasma density have been recently achieved at JET [1, 2]. A major drawback of the Type I ELMy H-mode is the periodic large energy losses associated with the Type I ELMs, which can lead to intolerable erosion rates when extrapolated to ITER [3, 4]. Hence, it is necessary to understand the physical mechanisms that determine the Type I ELM size in H-modes to assess whether the ELMy H-mode is a fully extrapolable regime to next step devices.

1. GLOBAL ELM OBSERVATIONS IN JET ELMY H-MODES

A common method for decreasing the ELM energy loss is with Deuterium gas puffing. Gas puffing decreases the ELM energy loss and increases the ELM frequency. In this way small ELMs are always seen at high ELM frequencies and with a deteriorated energy confinement [5]. New results in JET (2.5 MA/2.4-2.7 T, P_{NBI} = 14-17MW) for discharges at high triangularity ($\delta \sim 0.5$) show a clear deviation from this standard behaviour with the ELM frequency decreasing for the higher fuelling rates as shown in Fig. 1, while the fraction of the energy lost at the ELM (determined by the values of the diamagnetic energy just before the ELMs and, typically, 1ms after the ELM) remains constant ($\sim 3\%$) as shown in Fig. 2. Simultaneous with this "frequency anomaly" there is an increase of the Da signal in between ELMs reminiscent of that seen during Type II ELMs in ASDEX-U [1]. Figures 1 & 2 include, as well, data from Ar seeded H-modes in which the plasma radiation is increased by impurity puffing, which tends to decrease the ELM frequency. In this case (particularly at low n_e/low δ), the ELM energy drop is significantly smaller than the one expected ($\sim 15\%$) due the very low ELM frequency achieved in these discharges (~ 5Hz).

The effect of the ELM losses in the total power and particle balance is shown in Figs. 3 and 4. The average power flux due to the ELMs ($f_{ELM}*\Delta W_{ELM}$) is typically about 30-40% of the total input power for both low and high d at low gas puffing rates. However, with increasing puffing it can decrease to values of 10-20% for high δ discharges, while it reaches 50-60% for lower δ discharges. This indicates that (for $P_{INP} \sim 15$MW) the observed decrease of the stored energy at high densities is driven by ELM energy losses for low δ discharges, while for high d the in-between ELM losses dominate [1]. Similarly, discharges with Ar seeding show a lower ELM average power flux consistent with the larger radiation in the core plasma.

The ELM particle drop (ΔN_{ELM}), on the other hand, seems to be weakly dependent on the ELM frequency. The typical particle content drop (estimated by the volume integral of the Abel inverted density profile from interferometer measurements) during an ELM in JET is 1.5-3.0% of the total particle content over a wide range of conditions. Only Ar seeded discharges with low ELM frequency show a deviation from this with typical ELM particle drops of $\sim 7\%$. As a consequence, the ELM average particle outflux ($f_{ELM}*\Delta N_{ELM}$) is mainly determined by the ELM frequency, reaching its highest values for low δ discharges at high fuelling rates. Although more analysis is required, the measurements indicate that ELM particle losses play an important role in achieving high densities

in ELMy H-modes. Therefore, maintaining a moderate ELM frequency at high density (moderate ELM particle outflux) by either operating at high δ [1], high power [2] or with Ar seeding [6] is required to achieve high plasma densities in Type I ELMy H-modes with good confinement.

Analysis of measurements from several experiments had indicated that the ELM energy loss is well correlated with the collisionality of the pedestal plasma [4]. Such dependence has been confirmed in these JET experiments (see Fig. 5) for a broad parameter range and experiments ($\delta = 0.3 - 0.5$, Pellet triggered ELMs, and Ar seeded H-modes) for which the ELM frequency behaves either "normally" or in an "anomalous" way. This finding indicates clearly that the ELM energy loss is determined by the plasma parameters at the pedestal region and that the ELM frequency is a consequence of the size of the energy loss plus the in-between ELM transport, contrary to the previous understanding [5]. The dependence of ELM size on pedestal collisionality can be understood in two ways [3, 4]: a) the MHD mode that causes the ELM depends on collisionality such that its amplitude and/or radial extent decrease with collisionality; b) higher collisionality means longer characteristic times for energy flow along the field line such that the plasma is able to loose less energy (at higher collisionalities) during the period of the ELM-caused ergodisation of the field lines.

2. ELM ENERGY LOSS PHYSICS AND DETAILED MEASUREMENTS.

In JET, Type I ELMs affect typically the outermost 10 - 15cm of the plasma (10-20% of the minor plasma radius), as deduced from fast electron temperature measurements. Measurements of the plasma behaviour during the ELM crash show that the typical time scale of the electron temperature drop in the pedestal region is ~ 200µs and similar to the duration of the enhanced MHD activity associated to the ELM (see Fig. 7). After this fast energy loss, in low input power (~ 12MW) and discharges without deuterium puffing, a second phase with duration of ~ 500µs is seen during which the pedestal temperature continues decreasing slowly, resembling the phenomenology in compound ELMs but in a much faster time scale [7]. This second phase is not present at higher powers and/or with deuterium puffing, for which the ELMs are smaller.

From the measured temperature and density drop during an ELM it is possible to estimate how much of the energy lost during the ELM is due to the decrease of the temperature and how much to the expulsion of particles during the ELM (i.e., conductive vs. convective losses). Fig. 6 shows the results of such analysis that, for the case of JET ELMy H-modes, indicates that, although the temperature drop ELM (conductive losses) dominates the ELM energy loss over a range of conditions, the loss of energy associated with the particle expulsion is not negligible ELM (convective losses). A parameter that can influence the energy lost during the ELMs is the duration of the phase of enhanced MHD activity associated with the ELM (τ_{ELM}). In JET this parameter has been measured with Mirnov coils and found to be ~ 200µs not dependent on plasma density and δ (see Fig. 7) for given I_p/B_t. On the contrary, the amplitude of the Mirnov signal seems to decrease with increasing density and, correspondingly, ELM size. The independence of τ_{ELM} with pedestal density and the decrease of the Mirnov signal with density seem a general feature of Type I ELMs and has also been seen in DIII-D [8]. A first interpretation of the MHD measurements would indicate that the observed collisionality dependence of the ELM energy loss

is a result of the varying MHD amplitude with increasing density and not of the parallel energy transport during the ELM. However, collisional effects during ELMs have been identified for the first time during these JET experiments (see Figs. 8 & 9) by measurements of the ion flux and D_α at the inner and outer divertors with high time resolution (~ 10µs). For discharges with no deuterium fuelling (large ELMs and low pedestal collisionality) the ELM-associated particle pulse is seen at both divertors simultaneously. With increasing deuterium fuelling (smaller ELMs and higher pedestal collisionality) the ELM-associated particle pulse appears ~ 200 - 300µs earlier at the outer divertor than at the inner divertor. This time difference is consistent with the characteristic SOL parallel transport time if the ELM losses are concentrated at the outer midplane. Detailed analysis of a complete set of measurements (MHD signals, divertor particle fluxes, soft X-ray emission and IR divertor power deposition) will be carried out to elucidate if these collisional effects are the driving mechanism behind the ELM energy loss decrease at high densities or simply coincidental with the decrease of the ELM-associated MHD activity.

CONCLUSIONS.

New measurements of ELM energy and particle losses in JET have shown that the energy loss during an ELM is determined by the plasma parameters at the pedestal before the ELM crash. The ELM frequency is, therefore, a consequence of the ELM energy drop and the inter-ELM energy confinement. The relative (to the pedestal) ELM energy loss is well correlated with pedestal collisionality with the smaller ELMs (7% of W_{ped}) being obtained at the highest collisionalities. At present it is not yet clear if the collisionality dependence is a result of the change of the MHD activity or of the slowing down of parallel transport with increasing collisionality, as evidence for both hypotheses has been found in the experiments. More detailed analysis of the measurements is in progress to try and find out which is the physical mechanism behind the observed decrease of ELM size with collisionality. The extrapolation of the existing measurements of ELM energy losses to ITER following the two hypotheses leads to very different estimates for the ELM size in this device [4].

ACKNOWLEDGEMENTS

REFERENCES

[1]. G.Saibene, et al, this conference.

[2]. R.Sartori, et al., this conference.

[3]. G.Janeschitz, et al., Jour. Nuc. Mat. **290-293** (2001) 1.

[4]. A.Loarte, et al., IAEA-CN-77 ITERP/11(R),18th IAEA Conference, Sorrento, Italy, 2000.

[5]. G.M.Fishpool, Nuc. Fusion **38** (1998) 1373.

[6]. J.Ongena, et al., this conference.

[7]. H.Zohm, Plasma. Phys and Contr. Fus. **38** (1996) 105.

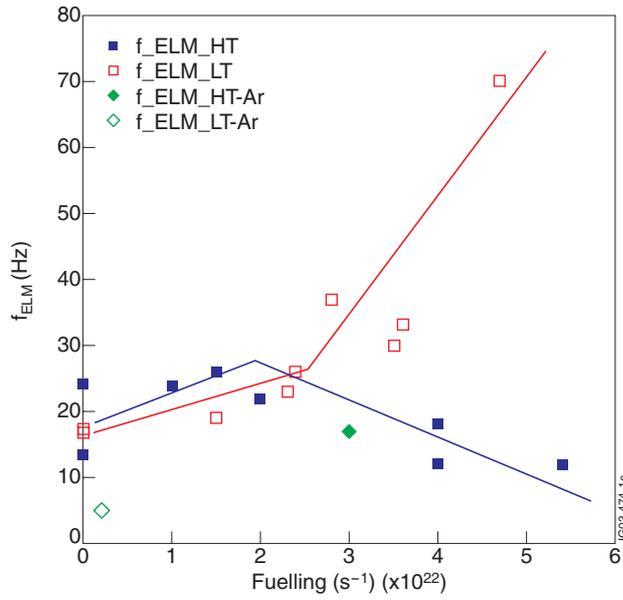[8]. A.Leonard, et al., Jour. Nuc. Mat. **290-293** (2001) 1097.

Figure 1: ELM frequency versus gas fuelling rate for similar discharges at low (0.3) and high δ (0.5) in JET. Two Ar seeded H-modes are shown for comparison.
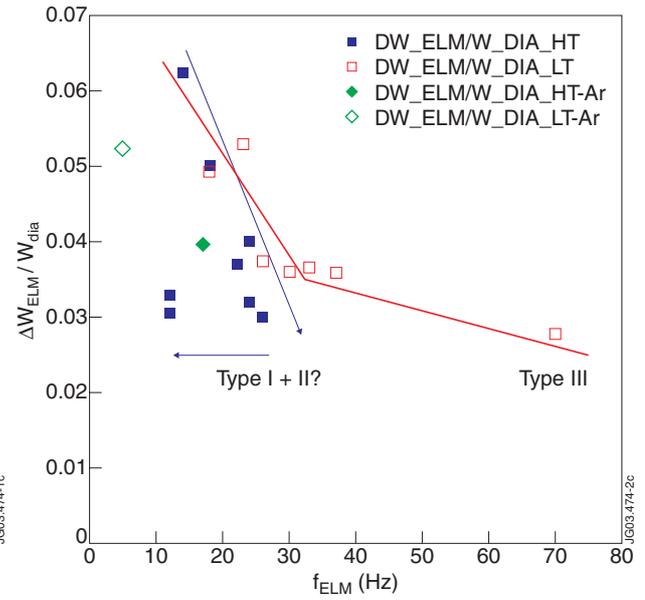

Figure 2: Fraction of plasma energy lost at the ELM versus frequency for similar discharges at low (0.3) and high δ in JET (0.5). Two Ar seeded H-modes are shown for comparison.
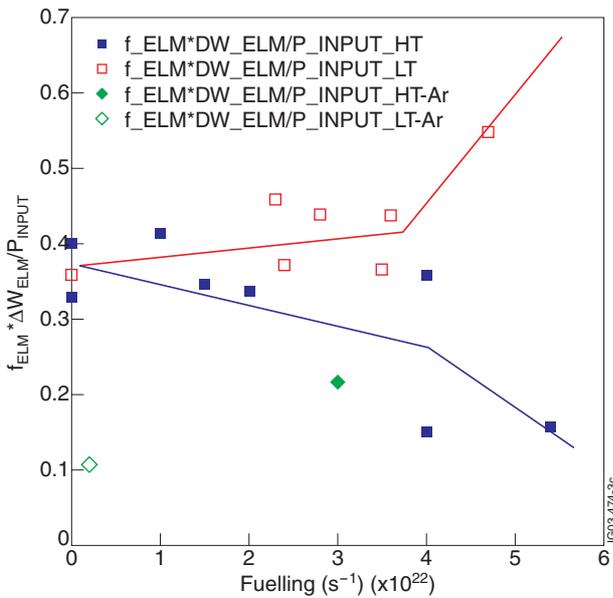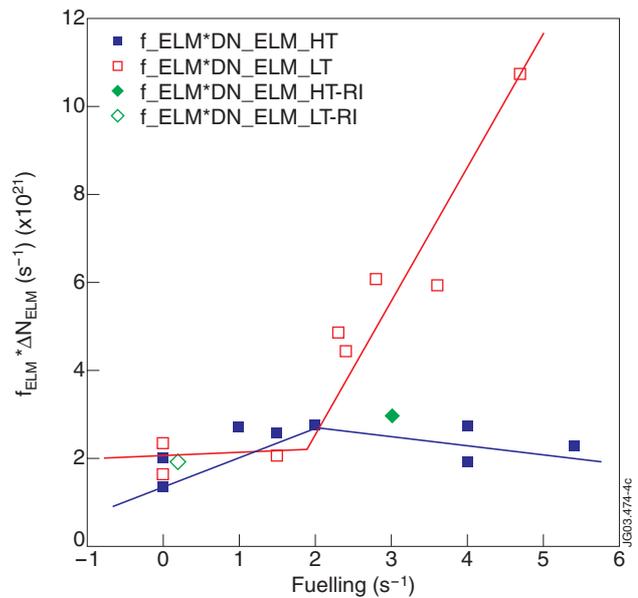

Figure 3: ELM average power flux versus fuelling rate for similar discharges at low (0.3) and high δ (0.5) in JET. Two Ar seeded H-modes are shown for comparison.

Figure 4: ELM average particle flux versus fuelling rate for similar discharges at low (0.3) and high δ (0.5) in JET. Two Ar seeded H-modes are shown for comparison.
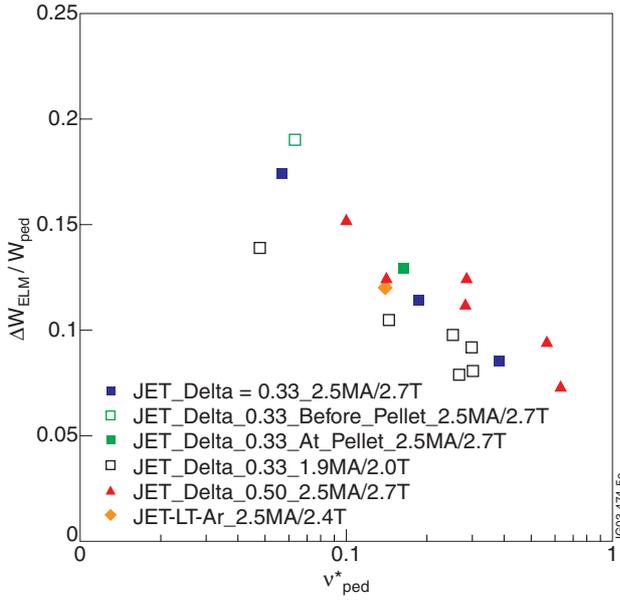
Figure 5: ELM energy loss normalised to the pedestal energy ($W_{ped} = 3 n_{e,ped} T_{e,ped} V_{plasma}$) versus parallel collisionality of the pedestal plasma for similar discharges at low (0.3) and high δ (0.5) in JET. The ELM energy losses for Ar seeded H-modes at low δ and for pellet triggered ELMs are shown for comparison.
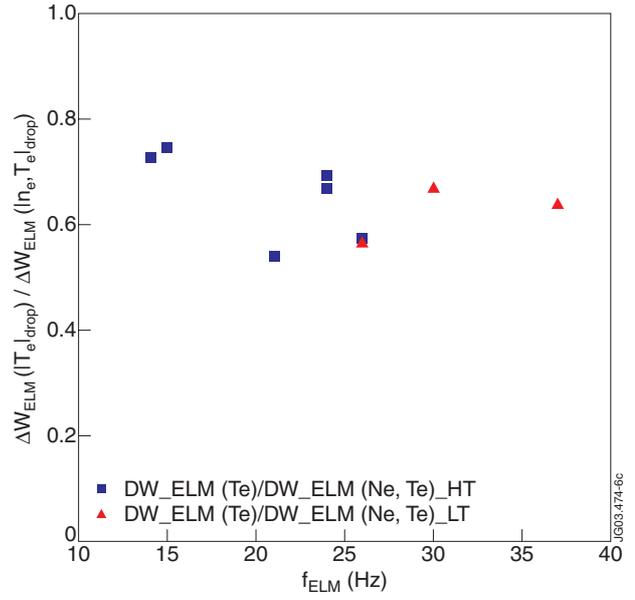

Figure 6: Proportion of the ELM energy loss with is lost due to the loss of temperature in the pedestal plasma versus ELM frequency for low (0.3) and high δ (0.5) ELMy H-modes.
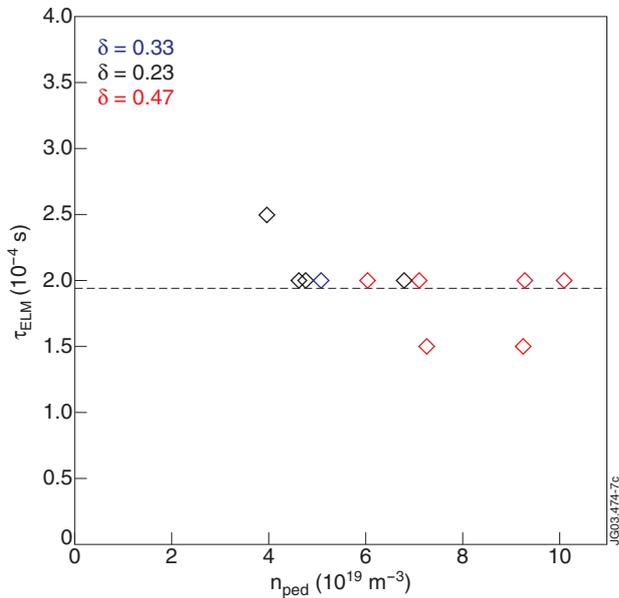

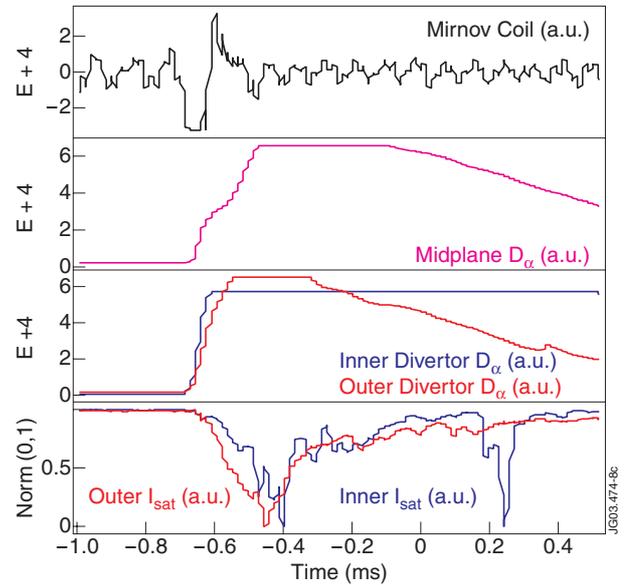*Figure 7: Period of enhanced MHD activity associated with the ELM versus pedestal density for discharges at various δ's.*

Figure 8: ELM measurements for a low density ELM. Top to Bottom : Mirnov coil signal. D_α emission from a horizontal chord at the midplane. D_α emission from the inner and the outer divertors. Ion flux (measured with Langmuir probes) at the inner and outer divertors.
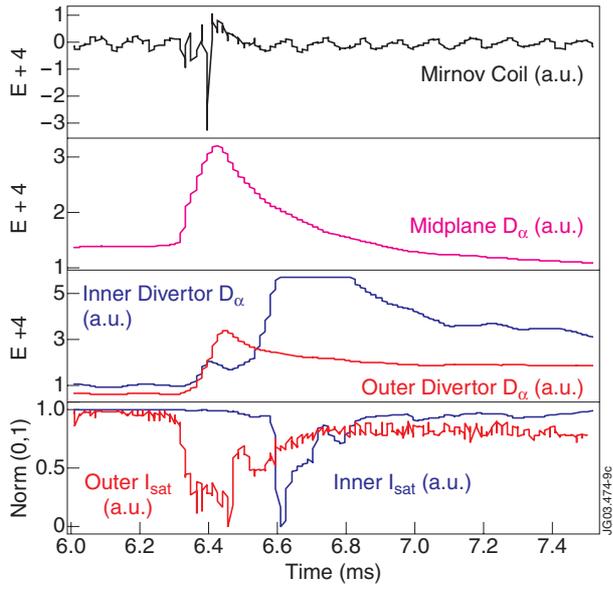
Figure 9: ELM measurements for a medium density ELM. Top to Bottom : Mirnov coil signal. D_α emission from a horizontal chord at the midplane. D_α emission from the inner and the outer divertors. Ion flux (measured with Langmuir probes) at the inner and outer divertors.